

Chlorine-Nuclear-Magnetic-Resonance Study of the Ferromagnet Gadolinium Trichloride^{*†}

Jan P. Hessler[‡]

Department of Physics, Michigan State University, East Lansing, Michigan 48823

(Received 29 January 1973)

We have utilized chlorine nuclear magnetic resonance to measure the magnetization as a function of temperature (0.032–4.2 K) and applied field (0–10 kOe) in the ferromagnet GdCl_3 . Above the Curie temperature, 2.214 K, there is only one ^{35}Cl pure-quadupole-resonance transition at 5314 kHz. Below the Curie temperature the internal field at the chlorine site splits the single transition line into three temperature-dependent transition lines. This observation is consistent with an internal field parallel to the symmetry axis C_3 . Analysis based on the method of energy moments yields a quadrupole asymmetry parameter of 0.4265 ± 0.0001 . The quadrupole Hamiltonian is diagonalized to give transition frequencies as a function of the pure-quadupole-resonance transition frequency, the asymmetry parameter, and the magnitude of the internal field. A least-squares analysis is used to determine the magnitude of the internal field as a function of temperature. With an external magnetic field applied parallel to the direction of the magnetization for a spherical sample, the critical point at the field $\vec{H}_{\text{int}} = \vec{H}_A - \vec{D} \cdot \vec{M}(T) = 0$ is used to measure the relationship between the internal field and the bulk magnetization. They are found to be simply proportional to within 0.5%, indicating a temperature-independent transferred hyperfine interaction. The transferred hyperfine field at the chlorine site is found to be antiparallel to the magnetization and equal to 1644 G at saturation. The zz component of the transferred hyperfine interaction tensor is 685 kHz for the ^{35}Cl nucleus. The zero-point magnetization defect $\Delta M_0/M_0$ is estimated at $(1.31 \pm 0.49)\%$. For $T < 0.5$ K the measurements show that the magnetization decreases faster than the predictions of Marquard and Stinchcombe and Cottam, based on the measured exchange constants. In the range $0.5 < T < 1.0$ K the internal field follows the equation $B(T) = 4956.9 - 868.1 T^{3/2} e^{-E_{\text{min}}/kT}$, where $E_{\text{min}}/k = 0.3586 \pm 0.0026$ K. Near the Curie temperature the critical exponent β is found to be 0.3904 ± 0.0060 with $T_c = 2.2140 \pm 0.0016$ K. The Green's-function predictions in the random-phase-approximation are compared to the magnetization measurements in zero and applied fields. The zero-field susceptibility is also calculated from the measurements.

I. INTRODUCTION

Gadolinium trichloride is a member of the small set of ferromagnetic insulators. Measurements of specific heat,¹ susceptibility, and magnetization^{1,2} indicate that it undergoes a phase transition to a ferromagnetic state at 2.2 K. The direction of magnetization is parallel to the symmetry axis C_3 . Electron-paramagnetic-resonance measurements³ have measured the Gd^{3+} -ion Zeeman splitting factor, and ion-pair spectra measurements^{4,5} have determined the form and magnitude of the exchange parameters. We report on measurements of the magnetization as a function of temperature and applied field. These experiments used the technique of nuclear magnetic resonance of both the ^{35}Cl and ^{37}Cl nuclei. Preliminary accounts of different parts of this work have been previously reported.^{6–8}

The normal procedure with accurate measurements of magnetization is to deduce the magnitude of the exchange parameters within the framework of an assumed model for the interaction and simplifying assumptions to make the calculations tractable.⁹ Because of the independent measurements of the exchange parameters we are in a position to compare our measurements with theoretical pre-

dictions based on these exchange parameters. GdCl_3 is well suited for such comparison because the exchange term is known to be isotropic with a dipole-dipole term of approximately equal magnitude.

In Sec. II we discuss the sample preparation and structure, the resonance spectrometer, and the low-temperature techniques. Section III is devoted to our zero-field resonance results. From the number of observed lines and symmetry we conclude that the internal field at the chlorine site is parallel to C_3 , the direction of the magnetization. The method of energy moments is used to measure the quadrupole asymmetry parameter. The nuclear-resonance Hamiltonian is diagonalized to give analytic functions for the transition frequencies. Results for the internal field as a function of temperature are then calculated.

Applied-field experiments are presented in Sec. IV which relate the magnetization to the internal-field measurements and show that they are simply proportional. A discussion of the zero-field measurements is presented in Sec. V. The critical exponent β is found to be 0.3904 and the critical region is consistent with high-resolution specific-heat measurements. Measurements below 0.5 K are compared to the calculations of

Marquard and Stinchcombe¹⁰ and of Cottam.¹¹ For the temperature range 0.5–1.0 K the magnetization follows the simple form $T^{3/2} e^{-E_{\text{min}}/kT}$. The results of the applied-field experiments are used to estimate the zero-point spin deviation at 1.31%. The transferred hyperfine interaction causes the internal field at the chlorine nucleus to be antiparallel to the magnetization and small as expected. In Sec. VI we discuss the measurements in an externally applied field. We present data of magnetization as a function of temperature and internal field. These results are compared to the Green's-function predictions in the random-phase approximation. Susceptibility results deduced from these measurements are also presented.

II. EXPERIMENTAL TECHNIQUE

A. Crystal Preparation and Structure

Anhydrous gadolinium trichloride was slowly melted under vacuum in a vertical Vycor tube. The impure polycrystalline sample was then distilled under vacuum into a Vycor tube suitable for use in a Bridgeman-Stockbarger furnace.¹² The lower tip of the sample tube was placed in the gradient of the furnace and observed until a single seed crystal was produced. The tube was then slowly lowered through the gradient and a clear single crystal was grown. No analysis of the stoichiometry or impurity content was attempted.

Because the crystals are hygroscopic, once they were removed from the growth tube they were stored and shaped under mineral oil. A protective coating of either Apiezon N grease or GE 7031 and toluene was used during the experiments. For the applied-field experiments a spherical sample of approximately $\frac{5}{8}$ -in. diameter was made by roughing out a sphere on a grinding wheel and lapping between two epoxy cones with fine grinding powder suspended in mineral oil. No deviation in diameter was detected using a vernier caliper.

Zachariasen¹³ has found the trichlorides of La through Gd to be hexagonal with space group $P6_3/m$. There are two molecules per unit cell. The locations of the rare-earth ions are determined by symmetry as being $\pm(\frac{1}{3}, \frac{2}{3}, \frac{1}{4})$ while the physically inequivalent chlorines are located at $\pm(u, v, \frac{1}{4})$, $(-v, u-v, \frac{1}{4})$, and $(v-u, -u, \frac{1}{4})$. Morosin¹⁴ has determined the room-temperature cell dimensions and the parameters u and v . He finds $a_0 = 7.3663 \pm 0.0009 \text{ \AA}$, $c_0 = 4.1059 \pm 0.0004 \text{ \AA}$, $u = 0.38929 \pm 0.00025$, and $v = 0.30153 \pm 0.00025$.

B. NMR and Field Measurements

All transition-frequency measurements were made using a simple pulsed spectrometer.¹⁵ We estimate the over-all accuracy of the transition-frequency measurements to be equal to the natural

linewidth of approximately 1 kHz. For accurate frequency measurements five independent readings were taken for each frequency. The standard deviation of these readings was generally less than 1 kHz.

To assure thermal equilibrium at low temperatures, the transition frequency with the largest dv/dT was measured at 10–20-min intervals while the temperature of the bath was maintained constant to within 0.2 mK. When two consecutive measurements of frequency agreed to within 0.5 kHz, the sample was assumed to be in thermal equilibrium with the bath.

For the applied-field experiments the sample was immersed directly in the ⁴He bath on a nylon goniometer which could rotate 360° about an axis in the plane of rotation of the externally applied field. The field was stabilized and measured to $\pm 0.1 \text{ G}$.

C. Temperature, Calibration, and Measurement

For experiments in the temperature range of 1.2–4.2 K, the sample was immersed directly in a ⁴He bath. A 200- Ω manganin resistor was used as a heater for fine control of the temperature below the λ point and as a stirrer above the λ point. The ⁴He vapor pressure¹⁶ was used as an absolute measure of temperature throughout the entire temperature range. The measured vapor pressure and sample temperature were strongly coupled as indicated by the fact that the temperature-dependent transition frequencies tracked the vapor pressure with little lag in time.

For the temperature range of 0.3–1.2 K a conventional ³He single-shot cryostat was used. The design follows closely that of Walton.¹⁷ Above 0.6 K the ³He vapor pressure was used to determine the temperature.¹⁸ Below 0.6 K the thermomolecular correction becomes significant, even for our large tube.¹⁹ Also dP/dT becomes small enough that pressure monitoring and measurement are not sensitive enough to keep temperature fluctuations on the order of 0.1 mK. Therefore, below 0.6 K, we used a germanium resistor for temperature measurement and a carbon resistor for temperature-fluctuation monitoring. Both resistances were measured independently by two Wheatstone bridges using a phase-sensitive detector operating at 33 Hz.

To calibrate the germanium resistor at low temperatures the magnetic temperature T^* of ferric ammonium alum was used as a standard. The mutual-inductance technique was used to determine the susceptibility.²⁰ The coils were calibrated using the vapor pressure of ³He as the temperature standard between 0.6 and 1.2 K. The relationship between T^* and T for $T > 0.2 \text{ K}$ is $(T^* - T) = 0.00548/T$ to within 0.1 mK.²¹

For temperatures below 0.3 K a ³He-⁴He mixing

refrigerator was used.²² The sample was immersed directly in the ³He-⁴He mixing chamber along with a carbon resistor for temperature measurement. The carbon resistor was calibrated on two independent runs with the susceptibility of a pressed cerium magnesium nitrate pellet as a temperature standard. We estimate the temperature uncertainty to be 5 mK.

III. ZERO-FIELD RESULTS

The Hamiltonian describing the interaction of a nucleus of spin $I \geq 1$ with the local magnetic field and electric field gradient may be written²³

$$\mathcal{H} = -\vec{\mu} \cdot \vec{B} - \frac{1}{2} \vec{Q} : \vec{\nabla} \vec{E} \quad (1)$$

The first term is the Zeeman interaction between the nuclear dipole moment $\vec{\mu}$ and the local magnetic field \vec{B} .²⁴ The second term is the quadrupole interaction between the nuclear quadrupole moment tensor \vec{Q} and the electric field gradient tensor (EFGT) $\vec{\nabla} \vec{E}$. We will use the xyz coordinate system which diagonalizes the field gradient tensor, $-(\nabla E)_{ij} = V_{ij} \delta_{ij}$ as our reference frame. The standard convention $|V_{xx}| \leq |V_{yy}| \leq |V_{zz}|$ defines the x , y , and z directions.

Because the chlorines are related by a threefold symmetry axis and inversion symmetry there is only one pure-quadrupole-resonance transition observed in the paramagnetic state. The fact that the chlorines lie on a mirror plane dictates that one of the principal axes of the EFGT must be parallel to C_3 . At the Curie temperature of 2.2 K, the ³⁵Cl pure-quadrupole-resonance transition at 5314 kHz splits into three observable temperature-dependent transition frequencies as shown in Fig. 1. The observation of only three transition frequencies and the crystalline symmetry are consistent with an internal field at the chlorine site which is parallel to C_3 . In all the rare-earth trichlorides La through Gd the x principal axis of the EFGT is parallel to C_3 .²⁵ We use the fact that \vec{B} is also along C_3 to greatly simplify our analysis of the observed spectra.

Before we can use the data of Fig. 1 to determine $B_{C_1}(T)$ we must deduce the value of the asymmetry parameter, η ; $\eta \equiv (|V_{yy}| - |V_{xx}|) / |V_{zz}|$. Brown and Parker²⁶ have applied the method of energy moments to the quadrupole Hamiltonian to derive analytic expressions for the energy moments in terms of polynomials which depend on the nuclear spin, the quadrupole coupling constant, the asymmetry parameter, and the magnitude and direction of the internal field. The moments of energy are defined as

$$S_1 = \sum_n \lambda_n, \quad S_2 = \sum_n \lambda_n^2, \quad \text{and} \quad S_3 = \sum_n \lambda_n^3. \quad (2)$$

The summation extends over the four energy levels λ_n . The first moment is equal to zero since the

representation is traceless. For our case the second and third moments reduce to

$$S_2 = \nu_Q^2 + 5\nu \quad (3a)$$

and

$$S_3 = (3\nu_Q \nu^2 / \rho)(\eta - 1). \quad (3b)$$

ν_Q is the pure-quadrupole-resonance frequency observed in the paramagnetic state. $\nu = \mu B / \hbar$ and $\rho = (1 + \frac{1}{3}\eta^2)^{1/2}$. Eliminating the field dependence and solving for η gives

$$\eta = [D \pm (D^2 - 4AC)^{1/2}] / 2A, \quad (4a)$$

where

$$A = \frac{9}{25} \nu_Q^2 (S_2 - \nu_Q^2) - \frac{1}{3} S_3^2, \quad (4b)$$

$$C = A - \frac{2}{3} S_3^2, \quad (4c)$$

and

$$D = 2A + \frac{2}{3} S_3^2. \quad (4d)$$

The energy levels in terms of the observed transition frequencies are given by

$$4\lambda_1 = -f_2 - 3f_3 + 2f_4, \quad (5a)$$

$$4\lambda_2 = -f_2 + f_3 - 2f_4, \quad (5b)$$

$$4\lambda_3 = -f_2 + f_3 + 2f_4, \quad (5c)$$

and

$$4\lambda_4 = 3f_2 + f_3 - 2f_4. \quad (5d)$$

f_2 is the highest observed zero-field transition frequency, f_3 the central, and f_4 the lowest. f_1 is not observed unless an external field is applied in the paramagnetic state. We find that η is temperature independent and equal to 0.4265 ± 0.0001 .

To determine the magnitude of the internal field as a function of temperature we diagonalize the quadrupole Hamiltonian to find the eigenvalues in terms of η , B_{C_1} , and ν_Q . Two eigenvalues are given by

$$\lambda_{\pm} = \frac{1}{2} \nu \pm \frac{1}{2} [\nu_Q^2 + 4\nu^2 - (\nu\nu_Q/2\rho)(1-\eta)]^{1/2}. \quad (6a)$$

The other two are

$$\lambda_{\pm} = -\frac{1}{2} \nu \pm \frac{1}{2} [\nu_Q^2 + 4\nu^2 + (\nu\nu_Q/2\rho)(1-\eta)]^{1/2}. \quad (6b)$$

The six transition frequencies are given by $f_i = \Delta\lambda_i$, where the eigenvalues are appropriately chosen. A least-squares analysis is used to determine $B_{C_1}(T)$. Both ³⁵Cl and ³⁷Cl transition frequencies are observed and used in the analysis.²⁷ Before we discuss the physical significance of these results in terms of the magnetization we investigate the relationship between $B_{C_1}(T)$ at a nuclear site and $M(T)$.

IV. RELATIONSHIP BETWEEN $B_{C_1}(T)$ AND $M(T)$

In the application of nuclear-resonance results to a discussion of magnetization, one generally

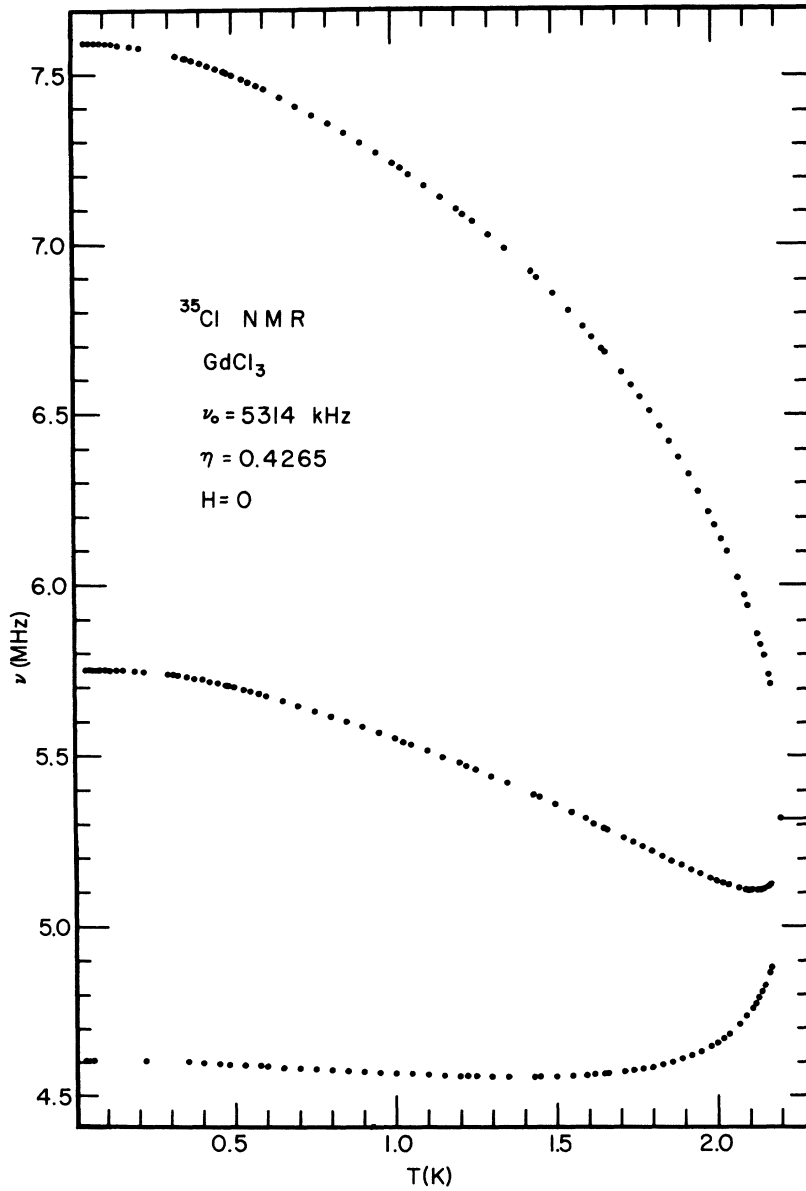


FIG. 1. ^{35}Cl nuclear-resonance transition frequencies as a function of temperature in the ferromagnetic phase of GdCl_3 . There is no externally applied field.

assumes that the \vec{B} field measured at the nuclear site is proportional to the magnetization. We have applied a rather well-known technique to test this assumption.

The spontaneous magnetization at a given temperature T is defined as

$$\vec{M}(T) = \lim_{\vec{H}_i \rightarrow 0} \vec{M}(\vec{H}_i, T), \quad (7)$$

where $\vec{M}(\vec{H}_i, T)$ is the magnetization appropriate to the internal field \vec{H}_i . \vec{H}_i is given by $\vec{H}_i = \vec{H}_A - \vec{D} \cdot \vec{M}(\vec{H}_i, T)$. \vec{D} is the classical demagnetizing factor and \vec{H}_A is the applied field. Wojtowicz and Rayl²⁸ have shown that for temperatures below the Curie temperature there exists a phase transition from a uniformly magnetized state to a nonuniform-

ly magnetized state at an applied field satisfying the relationship

$$\vec{H}_i = \vec{H}_A - \vec{D} \cdot \vec{M}(T) = 0. \quad (8)$$

Since nuclear resonance is sensitive to \vec{B} we note that for $\vec{H}_A < \vec{D} \cdot \vec{M}(T)$ any nuclear-resonance transition frequency will be independent of the applied field. For $\vec{H}_A > \vec{D} \cdot \vec{M}(T)$ the resonance frequency will be a function of \vec{H}_A . We stress that while the frequency of the nuclear-resonance transition depends on the microscopic parameters such as the internal field and the quadrupole interaction, the kink in a frequency versus applied-field plot will depend solely on the macroscopic parameters \vec{D} and $\vec{M}(T)$.

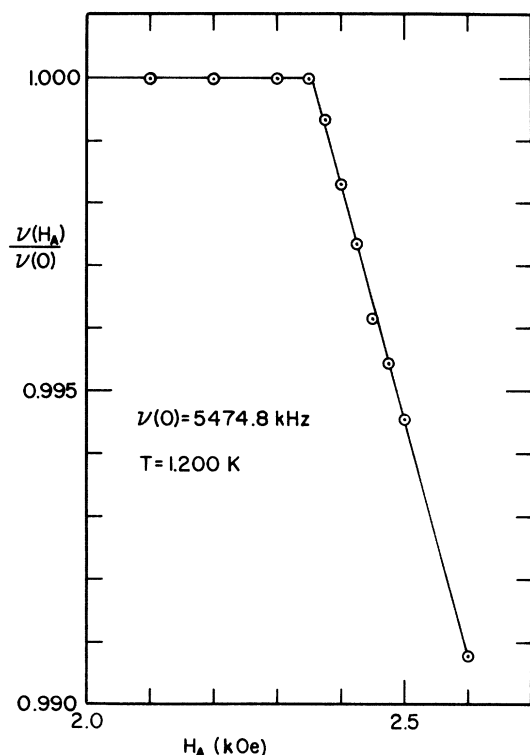


FIG. 2. Normalized ^{35}Cl nuclear resonance transition as a function of applied field. H_A is parallel to C_3 . The kink occurs at the critical field $H_C = \frac{4}{3}\pi M(T)$.

To utilize this technique on GdCl_3 we used a spherical sample for simplicity. Therefore $\bar{D} = \frac{4}{3}\pi$ and is independent of the applied-field orientation. We found that a very good sphere was necessary. In a poor sphere we could not observe the resonance signals up to the critical field, $H_C(T) = \frac{4}{3}\pi M(T)$. With a good sphere the resonance lines could be followed up to 10 kOe. At 10 kOe, we aligned the applied field along the C_3 axis by rotating both the sample and the magnetic field until the three nonequivalent chlorine resonance lines coalesced into a single line. The linewidth of this single line is comparable to the linewidth in zero applied field.

Figure 2 shows a plot of the normalized frequency, $\nu(H_A)/\nu(0)$, as a function of applied field for a single ^{35}Cl resonance line. Although we can measure the frequency to only 1 part in 10^4 , we can detect frequency shifts of the lines to 1 part in 10^5 . Below the critical field, $H_C(T)$, the nuclear-resonance transition frequencies are constant to within 1 part in 10^5 . We also note that we did not detect any hysteresis effects. Data were taken at small and large field differences approaching the critical field both from above and below. All data agreed to within the standard deviation of the frequency measurements.

TABLE I. Critical-field data used to measure the relationship between $B_{C1}(T)$ and $M(T)$. H_C is the field value of the kink in a frequency vs applied field plot. B_{C1} is the internal field at the chlorine site calculated from the measured transition frequencies.

$T(\text{K})$	$H_C(\text{Oe})$	$B_{C1}(\text{G})$	$K = 3H_C/4\pi B_{C1}$
1.2	2353 ± 10	4148.3 ± 2.0	0.13541 ± 0.00058
1.3	2280 ± 10	4020.9 ± 2.0	0.13537 ± 0.00060
1.4	2191 ± 10	3874.5 ± 3.0	0.13500 ± 0.00062
1.5	2094 ± 10	3712.5 ± 2.0	0.13465 ± 0.00065
1.6	1990 ± 10	3527.0 ± 3.0	0.13470 ± 0.00069
1.7	1880 ± 15	3312.4 ± 3.0	0.13550 ± 0.00109
1.8	1760 ± 30	3067.8 ± 2.5	0.13696 ± 0.00234
1.9	No critical field measured		
2.0	1335 ± 25	2396.4 ± 2.0	0.13299 ± 0.00250
2.1	1060 ± 20	1872.4 ± 5.0	0.13515 ± 0.00258

The results of data similar to that shown in Fig. 2 are presented in Table I. At each temperature we define the factor $K(T)$ by $K(T) = M(T)/B_{C1}(T)$. Table I shows that all $K(T)$ are equal within experimental error. A weighted average of all the data gives $K_{av} = 0.13509$ with a standard deviation of 0.00065. We therefore know that to within 0.5% the internal field measured at the chlorine site is simply proportional to the magnetization. The inability to measure a critical field near 1.9 K is due to the fact that at that temperature $\partial B_{cl}/\partial H_i$ at small H_i is very near zero. This is illustrated in Fig. 3, where we have plotted the normalized B , $B(H_A)/B(0)$, as a function of H_A for several temperatures.

The internal-field behavior as a function of tem-

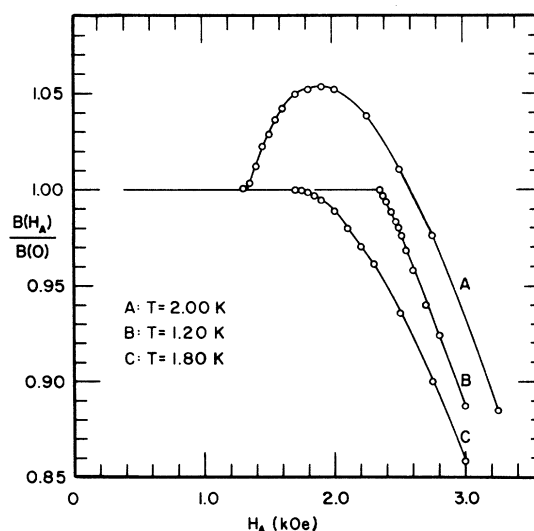


FIG. 3. Isothermal field dependence of the normalized internal field as a function of applied field. H_A is parallel to C_3 . The behavior indicates that the internal field at the chlorine site is antiparallel to the magnetization.

perature and applied field is explained in terms of a negative transferred hyperfine field from the gadolinium ions to the chlorine nuclei. The fact that the $T = 1.2$ K curve has a negative slope up to $H_A = 10$ kOe indicates that the direction of the spin of the Gd ion and the field on the chlorine nucleus are antiparallel. We then write the internal field as

$$B_{C1}(H_i, T) = -(1/K)M(H_i, T) + H_i. \quad (9)$$

Therefore,

$$\frac{\partial B_{C1}(H_i, T)}{\partial H_i} = -\frac{1}{K} \frac{\partial M}{\partial H_i}(H_i, T) + 1. \quad (10)$$

At low temperatures $(1/K) (\partial M/\partial H_i)$ is always less than 1 and we have the monotonic behavior shown. Just below the Curie temperature and for small H_i , $(1/K) (\partial M/\partial H_i)$ is greater than one. As H_i increases, $(1/K) (\partial M/\partial H_i)$ decreases and eventually becomes less than one. Therefore we have the behavior shown for $T = 2.0$ K.

A further conclusion based on the observation of the resonance signals at all applied fields up to 10 kOe is that the observed resonances are from the interior of the domains and not the domain walls. Signals from the domain walls would diminish as we increase the applied field and approach the critical field H_C . This is not observed. The signal amplitude remains approximately constant up to and through the critical field. Even at fields of 10 kOe where all the domain walls are removed we still observe strong resonances.

V. DISCUSSIONS OF ZERO-FIELD RESULTS

Since we have shown that the internal field measured at the chlorine site is simply proportional

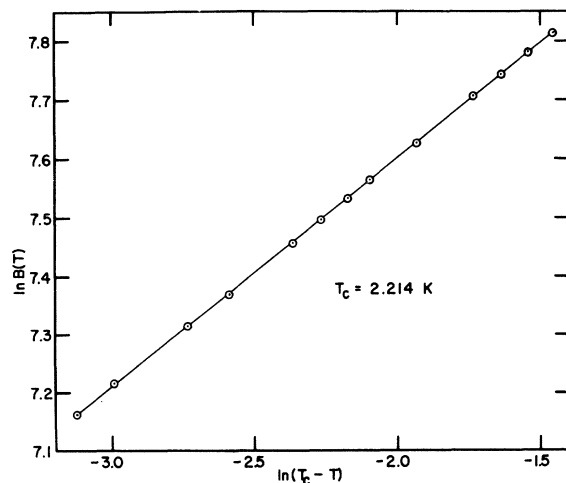


FIG. 4. Temperature dependence of the magnetization in the vicinity of the critical temperature. The reduced temperature range is $0.91 < T/T_C < 0.985$.

to the bulk magnetization to within 0.5%, we may compare our measurements to the various theoretical predictions for the magnetization.

A. Critical Region $T \lesssim T_C$

Domb and Sykes²⁹ and Fisher³⁰ have pointed out that in the vicinity of the transition the magnetization may be characterized by the relationship $M = A(T_C - T)^\beta$. T_C is the critical temperature and β is the critical exponent. Figure 4 shows a plot of $\ln B(T)$ as a function of $\ln(T_C - T)$ for $T > 1.980$ K. The critical parameters were determined by least-squares fitting the measurements to the equation $B_{C1}(T) = A(T_C - T)^\beta$. The results are $A = 4368 \pm 31$ G K $^{-\beta}$, $T_C = 2.2140 \pm 0.0016$ K, and $\beta = 0.3904 \pm 0.0060$.

Landau³¹ has made high-resolution specific-heat measurements and finds that the asymptotic form of the specific heat is *not* singular. The transition is of the "diffuse" type.³² However, he does find that there is critical-like behavior in the range $0.91 < T/T_C < 0.999$. Our results are consistent with this although we only have data up to $T/T_C = 0.985$. The measured value of β is consistent with other measurements on magnetic systems,³³ but both the molecular-field approximation and the Green's-function technique decoupled in the random-phase approximation predict $\beta = \frac{1}{2}$.

B. Spin-Wave Region, Temperature Dependence

In GdCl_3 the dipole-dipole term is comparable to the exchange term, therefore the spin-wave treatments of Holstein and Primakoff³⁴ do not apply. Marquard and Stinchcombe¹⁰ were the first to theoretically study the spin wave region of GdCl_3 . They generalized the interaction between spin operators to include any symmetric interaction. They found that if the minimum in the dispersion curve occurred at $|\vec{k}| = 0$, $\theta_k = 0$ (θ_k is the polar angle of \vec{k}) the magnetization would follow the relationship

$$\Delta M \propto T^{5/2} e^{-E_0/kT}. \quad (11)$$

$\Delta M \equiv (M_0 - \Delta M_0) - M(T)$, where M_0 is the saturation magnetization and ΔM_0 is the zero-point spin deviation. E_0 is the gap in the dispersion curve at $|\vec{k}| = 0$. They estimate $E_0/k = 0.4$ K. They also state that if the minimum in the dispersion curve is not at $|\vec{k}| = 0$, $\theta_k = 0$, the coefficient in the exponential will be reduced and the power in the temperature term will be different.

Recently, Cottam¹¹ has used a high-density perturbation method to calculate the magnetization, free energy, and spin correlation function for GdCl_3 . Using the exchange constants of Clover and Wolf³⁵ he finds the magnon dispersion relation to be highly anisotropic. The minimum energy gap is found to be at $|\vec{k}| = 0.28 \text{ \AA}^{-1}$, $\theta_k = 0$, with

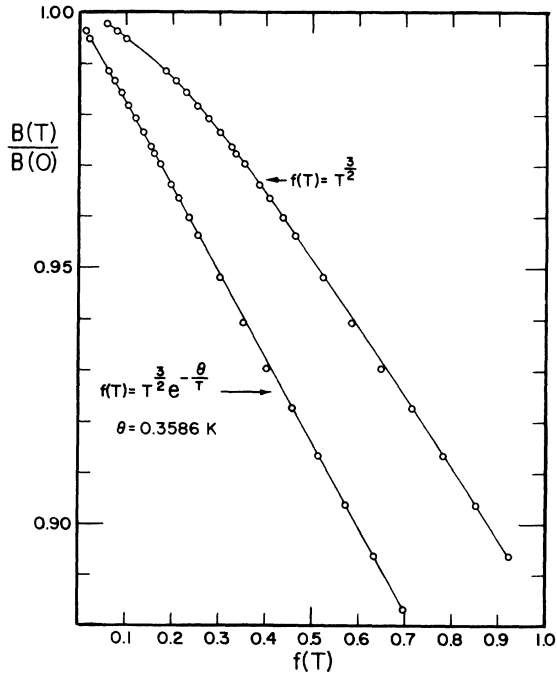


FIG. 5. Measurements of the reduced internal field for the temperature range 0.3–1.0 K. The data are plotted as a function of $f(T)$. For one case $f(T) = T^{3/2}$, for another $f(T) = T^{3/2} e^{-0.3586/T}$. $B(0)$ is assumed to be 4956.2 G.

$E_{\text{min}}/k = 0.36 \pm 0.03$ K. Carrying out a Taylor expansion about the minimum energy gap he finds

$$\Delta M \propto T^{7/4} e^{-E_{\text{min}}/kT}. \quad (12)$$

To measure the gap energy and the power of the temperature term we fitted our data to the various analytic expressions for several temperature intervals up to 1.0 K. For the temperature range $0.5 \leq T \leq 1.0$ K we found the internal field fits the expression

$$B(T) = B_0 - AT^{3/2} e^{-E/kT}, \quad (13)$$

where $B_0 = 4959.6 \pm 1.2$ G, $A = 868.1 \pm 2.4$ G K $^{-3/2}$, and $E/k = 0.3586 \pm 0.0026$ K. To illustrate this, Fig. 5 shows the reduced internal field as a function of $T^{3/2}$ and $T^{3/2} e^{-0.3586/T}$ for the temperature range 0.3–1.0 K. Above 1.0 K the internal field deviates from this behavior.

Because of the exponential term, measurements below 0.3 K could not be fit to a single analytic expression. To differentiate between a $T^{5/2}$, a $T^{7/4}$, or a $T^{3/2}$ term times an exponential would require an accuracy of at least two orders of magnitude better than can be achieved with NMR. We simply compare our results with the predictions of Marquard and Stinchcombe¹⁰ and Cottam.¹¹ This is done in Fig. 6. The results are normalized to agree with the zero-temperature magnetization predicted by Marquard and Stinchcombe.¹⁰ The

two theoretical predictions differ very little even though Marquard and Stinchcombe¹⁰ used $J_1/k = -0.0242$ K and $J_2/k = +0.0406$ K while Cottam¹¹ used the more recent values of $J_1/k = -0.039$ K and $J_2/k = +0.048$ K. The measurements are significantly different from the predictions. There is also no simple way to relate the measurements and the predictions.

C. $T = 0$, Zero-Point Magnetization Defect

Because the operator S^z does not commute with the Hamiltonian we do not expect the magnetization at $T = 0$ to be given by the usual formula $M_0 = 2g\mu_B S/V_{\text{cell}}$. Instead we expect a zero-point magnetization defect, ΔM_0 . In earlier work it was felt that this may have been as high as 10 or 15%.^{1,2} The spin-wave calculation predicts 0.19%,¹⁰ the high-density perturbation calculation predicts 0.16%,¹¹ and the Green's-function calculation predicts 0.5%.³⁶

With our experimental measurement of the proportionality between $B_{C1}(T)$ and $M(T)$ we calculate $M(0) = 669.5 \pm 3.2$ emu/cm³. Using the room-temperature cell parameters and the ion g value of 1.991 we have $M_0 = 669.9$ emu/cm³. We thus have that $\Delta M_0/M_0$ is zero within experimental error. For this calculation we have assumed there is no change in cell volume as the temperature is low-

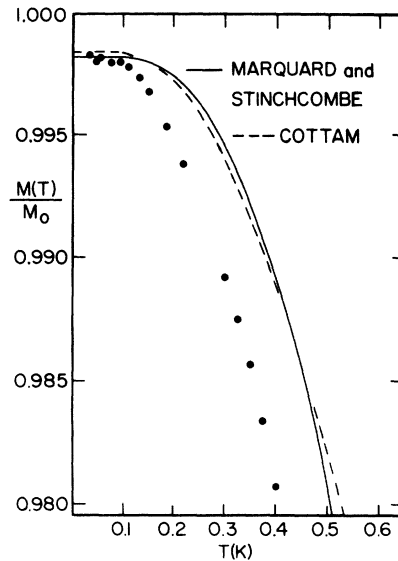


FIG. 6. Comparison of the measured reduced magnetization to the calculated. The measurements were normalized to agree with the $T = 0$ reduced magnetization of $M(0)/M_0 = 0.9981$ predicted by Marquard and Stinchcombe. The curve is for their set B values of the exchange constants $J_1/k = -0.0242$ K and $J_2/k = +0.0406$ K. Cottam's calculation uses the values $J_1/k = -0.039$ K and $J_2/k = +0.048$ K. The error in the measurements is approximately equal to the size of the black dots.

ered. Since there is no direct measurement of this change available we estimate the volume change from the temperature dependence of the pair spectra in LaCl_3 .

Birgeneau, Hutchings, and Wolf³⁷ have measured the temperature dependence of γ_{na} and γ_{ann} from 20 to 300 K. From their results we find that the c_0/a_0 ratio is temperature independent and that the cell volume decreases by approximately 1.25% as the temperature is lowered to 0 K. This implies that $M_0 = 678.4 \text{ emu/cm}^3$. Therefore, $\Delta M_0/M_0 = (1.31 \pm 0.49)\%$. Although this value is too uncertain to compare with theory, it is much smaller than the previously assumed value of 10–15%.

Knowledge of the cell parameters below the transition temperature would not necessarily help our analysis because we do not know the effective g value in the pure GdCl_3 salt. Very-low-temperature studies, 0.3 K, in very high fields, approximately 15 kOe, should allow for accurate measurements of ΔM_0 . Unfortunately with our present apparatus these were not possible.

D. Magnitude of the Transferred Hyperfine Interaction

It was pointed out in Sec. IV that the transferred hyperfine field at the chlorine nucleus is antiparallel to the magnetization. In the absence of an applied field we write the internal field at the i th chlorine nucleus as

$$\vec{B}_i = g\mu_B \sum_j \left(\frac{3\langle \vec{S}_j \rangle \cdot \vec{r}_{ij} \vec{r}_{ij}}{r_{ij}^5} - \frac{\langle \vec{S}_j \rangle}{r_{ij}^3} \right) - \frac{1}{\gamma_N \hbar} \sum_j \vec{A}_{ij} \cdot \langle \vec{S}_j \rangle. \quad (14)$$

The first term is the classical dipole contribution. The summation over j is over all gadolinium sites, $\langle \vec{S}_j \rangle$ is the mean value of the spin, and \vec{r}_{ij} is the vector from the i th chlorine to the j th gadolinium. The second term represents the transferred hyperfine field. \vec{A}_{ij} is the transferred-hyperfine-interaction tensor and γ_N is the nuclear gyromagnetic ratio. If we define the direction of magnetization as the z direction, Eq. (14) simplifies to³⁸

$$B_i^z = g\mu_B \langle S \rangle \sum_j \frac{3 \cos \theta_{ij} - 1}{r_{ij}^3} - \frac{1}{\gamma_N \hbar} \langle S \rangle \sum_j A_{ij}^z. \quad (15)$$

We actually measure A_0^{zz} defined as $\sum_j A_{ij}^z$. Using the Ewald technique³⁹ we find the dipolar sum to be equal to $+0.01154 \text{ \AA}^{-3}$. Therefore the dipolar field is 745.5 G for an assumed g value of 1.991. Assuming a saturation magnetization of 678.4 emu/cm^3 we have that $(\gamma_N \hbar)^{-1} A_0^{zz} = 1644 \text{ G}$. Thus $A_0^{zz}/\hbar = 685.0 \text{ kHz}$ or $A_0^{zz}/hc = 2.288 \times 10^{-5} \text{ cm}^{-1}$. These results refer to the ^{35}Cl nucleus.

The fact that the transferred hyperfine field is antiparallel to the Gd spin is consistent with all other results of rare-earth transferred hyperfine interactions.^{40,41} The relatively low magnitude is also consistent with previous work.

VI. APPLIED FIELD

A. Calculation of $M(H_i, T)$

Applying an external field along the direction of magnetization not only allows us to measure the relationship between $\vec{B}_{C_1}(T)$ and $\vec{M}(T)$ but also $\vec{M}(\vec{H}_i, T)$. Because \vec{B}_{C_1} , $\vec{M}(T)$, and \vec{H}_A are all collinear we may use the relationships discussed in Sec. III to deduce $\vec{B}_{C_1}(\vec{H}_A, T)$ from measured nuclear resonance transition frequencies as a function of \vec{H}_A and T . From Eq. (9) and the relationship $\vec{H}_i = \vec{H}_A - \vec{D} \cdot \vec{M}(\vec{H}_i, T)$ we have

$$M(H_i, T) = \frac{H_A - B_{C_1}(H_A, T)}{(1/K + D)}. \quad (16)$$

We must remember that for H_A just above the critical field H_C , $B_{C_1}(H_A, T)$ is negative. In

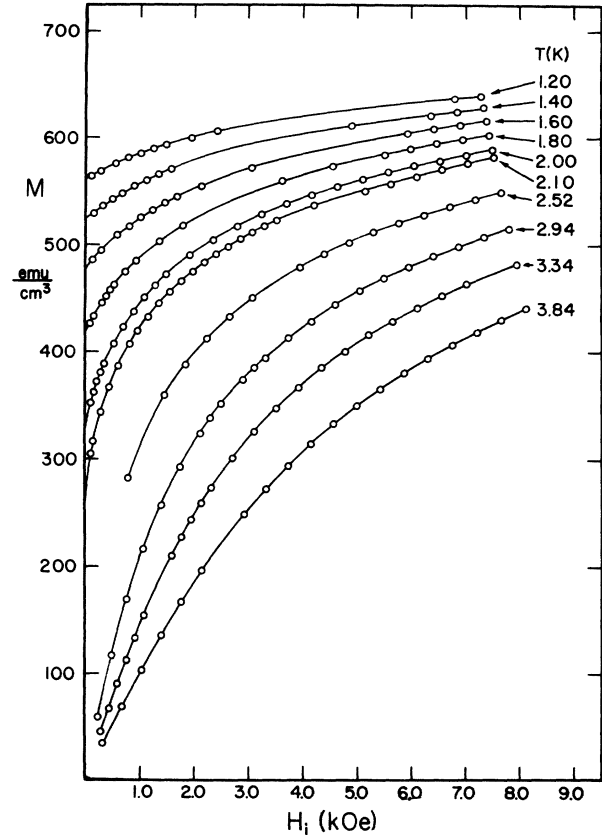


FIG. 7. Isothermal magnetization as a function of internal field. Calculation from internal-field measurements from the relationship $M(H_i, T) = H_A - B_{C_1}(H_A, T)/(1/K + D)$. H_A is parallel to C_3 . Accurate numerical data are available from Ref. 27.

TABLE II. Susceptibility results calculated from $M(H_i, T)$ measurements.

$T(K)$	$\chi(T) = \lim_{H_i \rightarrow 0} \frac{\partial M(H_i, T)}{\partial H_i}$ ($\times 10^{-3}$)
1.200	25.7 ± 0.5
1.300	36.6 ± 0.5
1.400	43.4 ± 1.0
1.500	61.2 ± 2.0
1.600	76.6 ± 4.0
1.700	93.0 ± 8.0
1.800	138.0 ± 10
2.943	246.0 ± 12
3.343	152.2 ± 2.5
3.843	100.2 ± 0.8

Fig. 7 we present the results of this analysis for several isotherms. Because nuclear resonance is a very sensitive probe we are also able to measure the magnetic susceptibility defined as

$$\chi(T) = \lim_{H_i \rightarrow 0} \frac{\partial M(H_i, T)}{\partial H_i}. \quad (17)$$

Results for susceptibility are given in Table II.

B. Comparison to Green's-Function Calculation

Becker and Plischke³⁶ have investigated the magnetization as a function of T and H for GdCl_3 using the technique of double-time thermodynamic Green's function⁴² in the random-phase-decoupling approximation. They derived a set of equations which may be solved self-consistently to give $S^z(T, H)$. These were solved numerically to determine $M(T, H)$.

The calculated $T=0$ magnetization is $0.995M_0$.

This is within the experimental error of our measurement. Using the exchange constants of Clover and Wolf³⁵ they calculate a critical temperature of $T_C = 2.48 \pm 0.12$ K. To compare their results to our measurement we have simply scaled their temperature to agree with the experimentally measured critical temperature. For $H_i = 0$ this scaling is valid since it is equivalent to the concept of a reduced temperature scale. For the field-dependent magnetization they have varied the magnetic field from 0 to 1 in units of $M_0/\mu_0 = 8440$ Oe. A comparison between the calculation and our measurement is shown in Fig. 8.

The agreement between the calculation and measurement is qualitatively good. Upon close examination of the $H=0$ case there are significant discrepancies. The exact reason for these may lie in the crudeness of the random-phase approximations, but this point must be investigated more thoroughly.

VII. CONCLUSIONS

The assumption that the internal field at a nuclear site is directly proportional to the magnetization of the sample is shown to hold in GdCl_3 . The nuclear-resonance "kink" method provides a very easy and accurate means of measuring the magnetization and the susceptibility. The limiting factors of this method are: (i) the temperature stability must be sufficient to satisfy the requirement that $\Delta T \partial \nu / \partial T|_T$ be less than the line width and (ii) the details of $\partial B / \partial H_i$ as $H_i \rightarrow 0$ must allow for an appreciable $\partial \nu / \partial H_i|_T$. The first is especially important near T_C where $\partial \nu / \partial T$ becomes very large. The latter depends on the sign and magnitude of the transferred-hyperfine field and

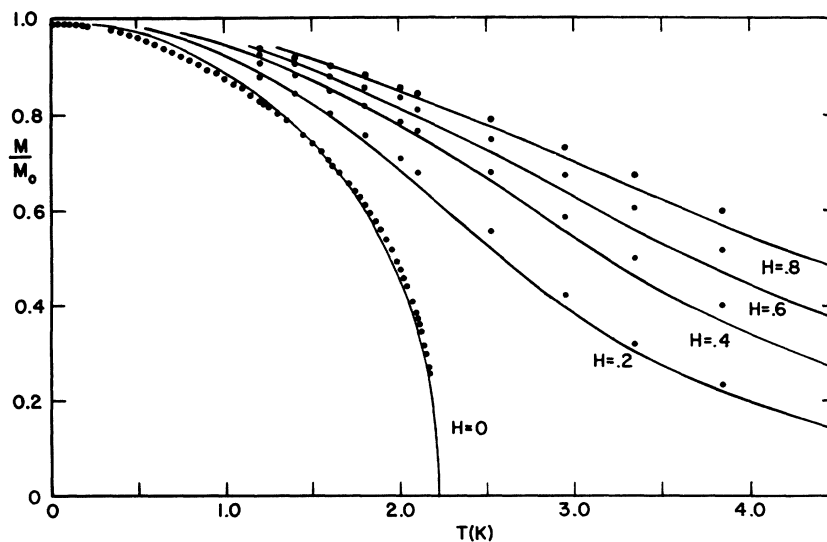


FIG. 8. Comparison of the measured $M(H_i, T)$ with prediction of Green's-function technique decoupled in the random-phase approximation. The lines are the calculation, the dots are the measurements. H is in units of $M_0/\mu_0 = 8440$ Oe. The temperature has been scaled to make the theoretical critical temperature of 2.48 K agree with the measurements.

the particular system under investigation.

The temperature dependence of the magnetization in the spin-wave region is consistent with the calculated minimum energy of the magnon dispersion curve. The direct comparison between the measurement and the calculations based on the measured exchange constants for $T < 0.5$ K indicate that further investigation is necessary. Nuclear-resonance studies in an applied field perpendicular to the direction of magnetization are also possible.

ACKNOWLEDGMENTS

It is a pleasure to acknowledge the guidance of Professor Edward H. Carlson, who served as my research advisor. He initiated this work and helped at every phase of its completion. I also wish to thank Robert D. Spence, Thomas A. Kaplan, and David H. Current for helpful discussions. I thank J. A. Cowen for the use of his ^3He - ^4He mixing refrigerator. Dennis E. Gallus and Peter Forney grew the crystals.

*Research supported by the U. S. Atomic Energy Commission.

[†]Some equipment used was purchased with a National Science Foundation Science Development Grant.

[‡]Present address: Enrico Fermi Institute and Department of Chemistry, University of Chicago, Chicago, Ill. 60637.

¹A. F. G. Wyatt, thesis (Oxford University, 1963) (unpublished).

²W. P. Wolf, M. J. M. Leask, B. Mangum, and A. F. G. Wyatt, *J. Phys. Soc. Jap. Suppl.* **17**, 487 (1961).

³C. A. Hutchison, Jr. and E. Wong, *J. Chem. Phys.* **29**, 754 (1958).

⁴R. J. Birgeneau, M. T. Hutchings, and W. P. Wolf, *J. Appl. Phys.* **38**, 957 (1967).

⁵M. T. Hutchings, R. J. Birgeneau, and W. P. Wolf, *Phys. Rev.* **168**, 1026 (1968).

⁶Edward H. Carlson, *Bull. Am. Phys. Soc.* **11**, 377 (1966).

⁷Jan P. Hessler, *Bull. Am. Phys. Soc.* **16**, 628 (1971).

⁸Jan P. Hessler, *Bull. Am. Phys. Soc.* **18**, 113 (1973).

⁹C. H. Cobb *et al.*, *Phys. Rev. B* **5**, 1677 (1971).

¹⁰C. D. Marquard and R. B. Stinchcombe, *Proc. Phys. Soc. Lond.* **92**, 665 (1967).

¹¹M. G. Cottam, *J. Phys. C* **5**, 2205 (1972).

¹²W. D. Lawson and S. Nielsen, *Preparation of Single Crystals* (Butterworths, London, 1958), Chap. 2, p. 14.

¹³W. H. Zachariasen, *Acta Crystallogr.* **1**, 265 (1948).

¹⁴B. Morosin, *J. Chem. Phys.* **49**, 3007 (1968).

¹⁵S. I. Parks, thesis (Florida State University, 1967) (unpublished).

¹⁶F. G. Brichwedde, 1958 *He Scale of Temperatures*, Natl. Bur. Stds. Monograph No. 10 (U.S. GPO, Washington, D.C., 1970).

¹⁷D. Walton, *Rev. Sci. Instrum.* **37**, 734 (1966).

¹⁸R. H. Sherman, S. G. Sydorik, and T. R. Roberts, Report No. LAMS-2701, 1962 (unpublished).

¹⁹A. Freddi and I. Modena, *Cryogenics* **8**, 18 (1968).

²⁰W. R. Abel, A. C. Anderson, and J. C. Wheatley, *Rev. Sci. Instrum.* **35**, 444 (1964).

²¹S. G. Sydorik and T. R. Roberts, *Phys. Rev.* **106**, 175 (1957).

²²John C. Wheatley, O. E. Vilches, and W. R. Abel, *Physics*

(L.I. City N.Y.) **4**, 1 (1968).

²³C. P. Slichter, *Principles of Magnetic Resonance* (Harper and Row, New York, 1963), Chap. 6.

²⁴We are dealing with the field inside a locally magnetized material therefore we use the symbol \vec{B} .

²⁵E. H. Carlson and H. S. Adams, *J. Chem. Phys.* **51**, 388 (1969).

²⁶L. C. Brown and P. M. Parker, *Phys. Rev.* **100**, 1764 (1955)

²⁷For detailed numerical values of transition frequencies, calculated internal fields, and error analysis, order NAPS Document No. 02111 from ASIS National Auxiliary Publications Service, c/o CCM Information Sciences, Inc., 305 East 46th Street, New York, N. Y. 10017; remitting in advance \$1.50 for microfiche or \$7.70 for photocopies.

²⁸P. J. Wojtowicz and M. Rayl, *Phys. Rev. Lett.* **20**, 1489 (1968); *Phys. Lett. A* **28**, 142 (1958).

²⁹C. Domb and M. F. Sykes, *Phys. Rev.* **128**, 168 (1962).

³⁰M. E. Fisher, *Rep. Prog. Phys.* **30**, 615 (1967).

³¹D. P. Landau, *J. Phys. (Paris)* **32**, 1012 (1971).

³²B. Pippard, *Classical Thermodynamics* (Cambridge U. P., London, 1957).

³³H. Eugene Stanley, *Introduction to Phase Transitions and Critical Phenomena* (Oxford U. P., New York, 1971).

³⁴T. Holstein and H. Primakoff, *Phys. Rev.* **58**, 1098 (1940).

³⁵R. B. Clover and W. P. Wolf, *Solid State Commun.* **6**, 331 (1968).

³⁶E. Becker and M. Plischke, *Phys. Rev. B* **1**, 314 (1970).

³⁷R. J. Birgeneau, M. T. Hutchings, and W. P. Wolf, *Phys. Rev. Lett.* **17**, 308 (1966).

³⁸We have changed notation; the present z direction was called the x direction in the EFGT reference frame.

³⁹D. B. Dickmann and G. E. Schacher, *J. Comput. Phys.* **2**, 87 (1967).

⁴⁰W. B. Lewis, J. A. Jackson, J. F. Lemons, and H. Taube, *J. Chem. Phys.* **36**, 694 (1962).

⁴¹A. J. Freeman and R. E. Watson, *Phys. Rev. Lett.* **6**, 277 (1961)

⁴²D. N. Zubarev, *Usp. Fiz. Nauk* **71**, 71 (1960) [*Sov. Phys.-Usp.* **3**, 320 (1960)].